Microchim Acta (2008) 160: 315–325
DOI 10.1007/s00604-007-0806-z
Printed in The Netherlands

Microchimica Acta

Review

Colloidal nanocrystal solar cells

Sandeep Kumar, Gregory D. Scholes

Lash Miller Chemical Laboratories, University of Toronto, Toronto, ON, Canada

Received 20 November 2006; Accepted 9 May 2007; Published online 16 July 2007

Abstract. Colloidal nanocrystal based organic solar cells are envisaged to be a cost effective alternative to conventional inorganic cells. A variety of studies have been reported recently with the goal to increases energy conversion efficiencies, which must be pushed towards 10% for devices to be practical. We review the status of this work, critically examining the factors affecting hybrid solar cell performance, and conclude with an outlook for future directions of research.

Keywords: Nanocrystal; solar; quantum dot

The growing world energy demands, limited fossil fuel resources, as well as considerations based on greenhouse gas emissions, are motivating the search for viable renewable energy sources. Among the possibilities, solar energy conversion is of great interest because it is globally available, inexhaustible, and electrical energy can be converted to other energy currencies such as hydrogen. Conventional inorganic semiconductor solar cells routinely exhibit a power conversion efficiency of 10% and in the best case up to ∼34% [1]. However, despite the good performance of these materials, their application is limited by the high cost of their fabrication, which involves elevated temperatures, numerous lithographic steps, and discrete processing due to the glass carriers.

Correspondence: Sandeep Kumar, Lash Miller Chemical Laboratories, University of Toronto, Toronto, ON, M5S 3H6, Canada, e-mail: skumar@chem.utoronto.ca

Colloidal quantum dots have been proposed as a cost effective alternative for developing hybrid solar cells because of their excellent solution processing ability, well-suited optical properties, and compatibility with conjugated polymers. These materials possess some of the desirable properties of bulk inorganic semiconductors, but are easily processed, like polymers. Most of the reports to date of photovoltaic devices based on colloidal quantum dots are hybrid polymer-nanocrystal designs. The polymers can be solution processed and their good mechanical properties enable flexibility of shape and size.

The operation of such solar cells is based on electrochemical principles where a photoactive layer is sandwiched between two electrodes of differing work function. The efficient performance of a solar cell depends primarily on the charge generation and subsequent transport to the respective electrodes. Efficient collection of charge carriers requires that the excitons created by the primary excitation be separated into charge carriers and be efficiently transferred to the respective electrodes; minimizing losses due to recombination. Most of the conjugated polymers investigated so far are intrinsic semiconductors, and the primary excitation in these cases is a nanoscale exciton [2]. It has been found that excitons in conjugated polymers can diffuse up to a distances of ∼10–15 nm [3–6]. That, in combination with the observation that hole, and particularly electron mobilities are low in conjugated polymers ($\sim 10^{-4}$ V cm^{-2} sec^{-1}) [7], means

that efficient devices need to be very thin. Fortunately the high absorption coefficient of conjugated polymers allows devices to be only a few hundreds of nanometer thick to exhibit efficient absorption cross-sections.

Charge separation in conjugated polymers has been found to be enhanced at the interface with materials of high electron affinity [8–10]. In addition to this, the low exciton diffusion distance of conjugated polymers demands a nanostructured interface. While several strategies are currently being pursued, such an interface is provided by colloidal quantum dots dispersed in a conjugated polymer host. These semiconductor nanoparticles have a high electron affinity relative to conjugated polymers, and thereby act as an electron acceptor. Although there have been a variety of research going on nanocrystal based solar cells, in this review we will focus our attention on colloidal nanocrystal based solar cells; that is, nanocrystal-polymer hybrids. We present the operating principle, state of art in the development of these types of solar cells, and conclude with an outlook for future research.

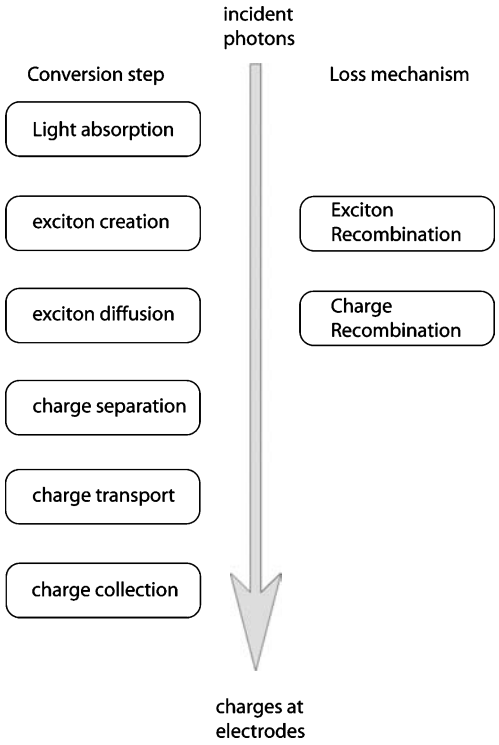

Fig. 1. Schematic flow chart showing the important processes in molecular and nanocrystalline solar cells. Recombination of excitons can be both radiative and non radiative

Basic processes of light harvesting in molecular solar cells

Solar energy is converted to electrical potential by a sequence of events: the absorption of light, generation of charge carriers (electrons and holes), and the transport of charge carriers to electrodes. However, for solar cells based on molecular systems such as polymers, this basic scheme needs to be developed further in order to explain photovoltaic performance. In bulk inorganic semiconductors, the binding energy of an exciton is close to thermal energies, and as such, the absorption of light leads essentially to separated, free charge carriers [11, 12]. However, because the exciton binding energy is substantial in molecular systems such as conjugated polymers or nanocrystals [2], the creation of carriers after light absorption is divided into three stages. Firstly, there is creation of a nanoscale exciton, the nature of which is different in conjugated polymers and inorganic nanocrystals compared to bulk inorganic semiconductors [13–17]. Secondly, the exciton dissociates, which likely occurs at the interface between two materials [18–22]. In case of nanocrystal based polymeric photovoltaic devices, the electron affinity and ionization potential between nanocrystal and polymer is one determining factor in the rate of that charge transfer. In the third stage, the separated charges are transported to the respective electrodes. The transport of charges occurs by diffusion assisted by the electric field generated from the difference in work functions of the electrodes [23–26].

A schematic of processes taking place in a polymer based photovoltaic cell is shown in Fig. 1. At each step, recombination of electron and hole can occur, preventing their contribution to the external current. In addition to the fundamental restrictions of the device, such as how much light can be absorbed, these recombination losses limit the overall maximum efficiency of the device and hence need to be minimized by all possible means.

The efficient operation of these hybrid solar cells depends on thermodynamic as well as kinetic factors. The thermodynamic requirements are that the energy levels of the components should be aligned in a way that the excitons created upon irradiation of the sample should be broken into separate charge carriers which should further be transported to the respective electrodes minimizing the possibility of their recombination in every possible way. Therefore, the ionization potential and electron affinity of the components play an important role in exciton dissociation, while the electron and hole mobility of the component defines

the ease of their transportation. Because of the small exciton diffusion distance in conjugated polymers, the morphology or interface in the hybrid films becomes an important factor for device performance.

The main reason for the superior efficiency of inorganic over organic devices lies in superior carrier mobilities. For most of conjugated polymers, electron mobilites are extremely low, typically well below $10^{-4}\,cm^2\,V^{-1}\,sec^{-1}$ [27]. Therefore, polymeric photovoltaic often rely on the introduction of another material such as nanocrystals for electron transport.

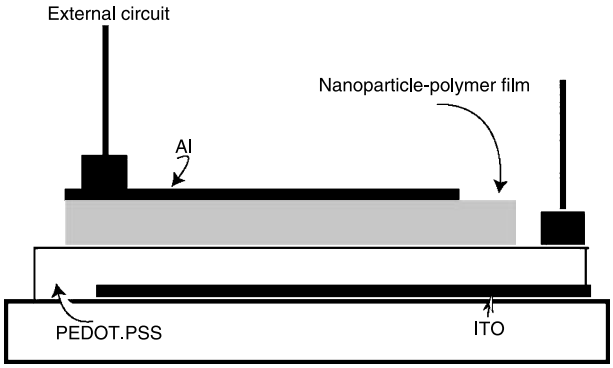

Fig. 3. Schematic of a typical nanocrystal-polymer hybrid solar cell

Material concept

The sun delivers an enormous amount of energy to the earth's surface, which at peak power, is approximately 1 $GW\,km^{-2}$. The solar radiation is emitted from the sun's photosphere at 6000 K temperature, which gives it a spectral distribution resembling closely that of a black body at the corresponding temperature. Passing through the earth's atmosphere the solar radiation is attenuated by scattering from molecules, aerosols and dust particles, as well as by absorption, in particular by oxygen, ozone, water vapor, and carbon dioxide. This gives a characteristic fingerprint to the solar radiation spectrum on the earth's surface as shown in Fig. 2.

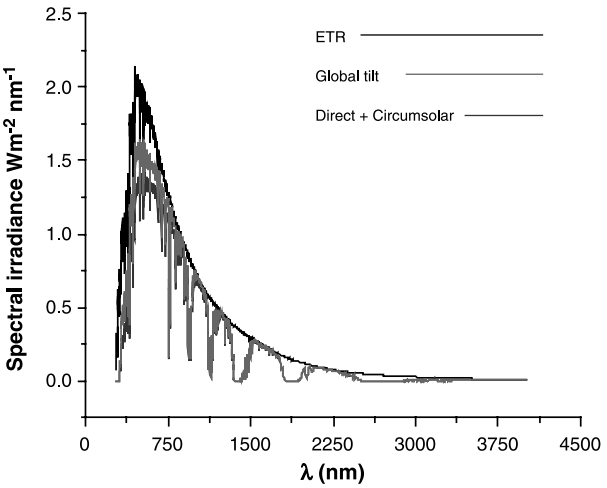

Fig. 2. The standard air mass (*AM*) 1.5 global solar spectrum. ETR is extraterrestrial radiation, also known as "top-of-atmosphere" (*TOA*) irradiance, is the amount of global horizontal radiation that a location on Earth would receive if there was no atmosphere or clouds (i.e., in outer space). Direct represents Direct Normal Irradiance nearly parallel (0.5° divergent cone) radiation on surface with surface normal tracking (pointing to) the sun, excluding scattered sky and reflected ground radiation. Circumsolar shows Spectral irradiance within ±2.5° (5° diameter) field of view centered on the 0.5° diameter solar disk, but excluding the radiation from the disk. Global Tilt displays spectral radiation from solar disk plus sky diffuse and diffuse reflected from ground on south facing surface tilted 37° from horizontal. Reprinted from Ref. [28]

Solar cells harness this energy by absorbing sunlight and converting it to an electrical power in the form of photogenerated current and voltage, and therefore, one of the most important criteria for designing a new solar cell is to consider the efficient absorption of the sun's radiation.

There has been numerous reports on nanocrystal-polymer hybrid solar cells based on CdSe [35–39], CdTe [41], PbS [42, 43], PbSe [44, 45], ZnO [52–54], and TiO_2 [55–58] nanocrystals and a variety of polymers namely P3HT, MEH-PPV and their various derivatives. In the following discussions, we will briefly discuss the state of art of solar cells based on these nanoparticle-polymer hybrids.

It was in 1996 when Greenham et al. first tried to incorporate CdSe nanocrystals in MEH-PPV but the power conversion efficiency was very low of the order of 0.01% [29]. In these devices the surface of the nanocrystals plays an important role in determining charge transfer from polymer to nanocrystal, and hence the power conversion efficiencies. It was observed that by derivatizing the nanocrystal surface with pyridine the nanocrystals are brought closer to the polymer, yielding better charge transfer and higher power conversion efficiency. The presence of pyridine ligands at the surface of the nanocrystals can facilitate the charge transfer process from polymer to nanocrystal by providing a low barrier distance between the nanocrystal and the polymer which otherwise is high when tri-n-octylphosphine oxide (TOPO) or other conventional ligands are present. Further, annealing these composite films can remove the surface bound pyridine (because of its high volatile character) and

possibly bring the nanocrystals in direct contact with the polymer, enhancing the charge transfer process significantly.

The real breakthrough in these nanoparticle-polymer hybrid devices followed the synthetic work of Peng et al. where shape anisotropy was introduced

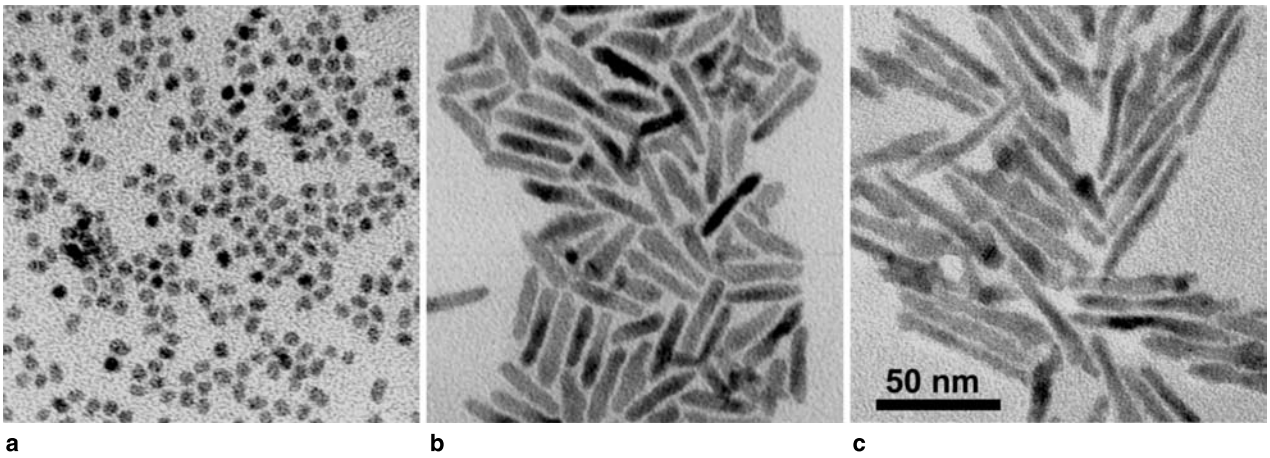

Fig. 4. (a–c) TEM images of different shaped CdSe nanocrystals. Reprinted with permission from Ref. [36]

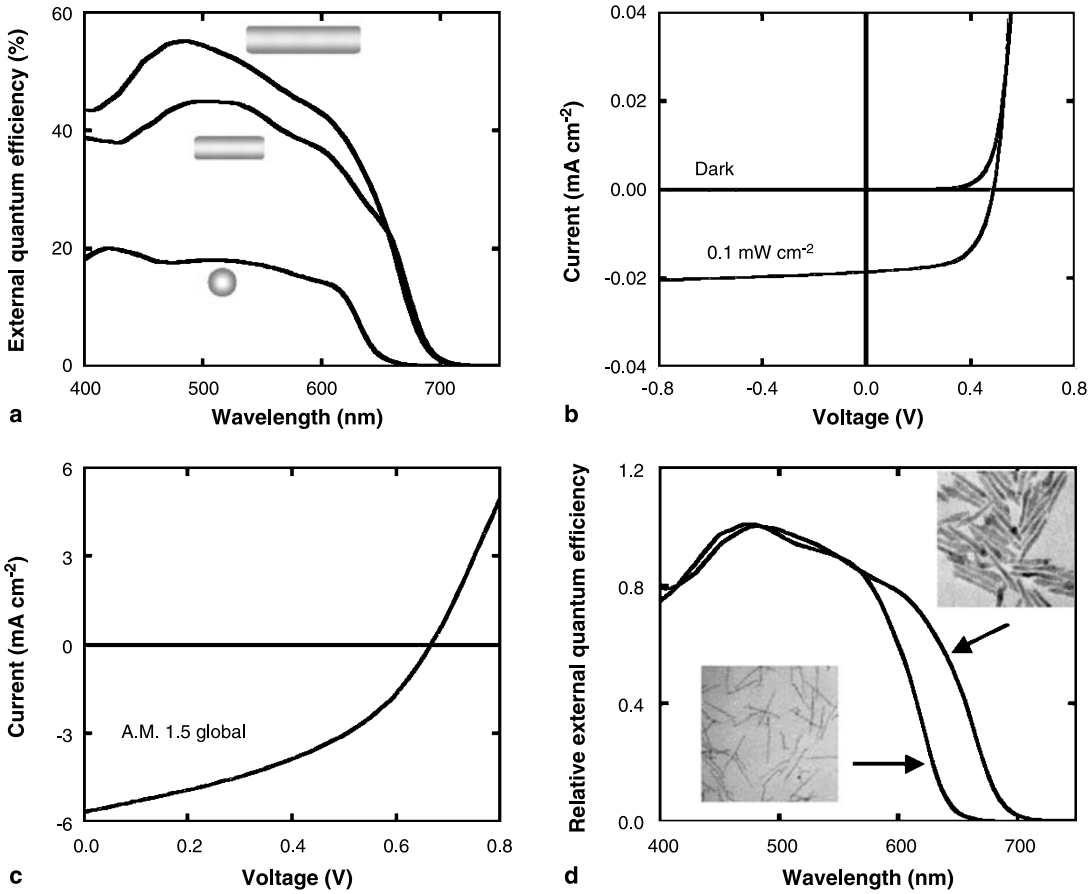

Fig. 5. (a) EQEs of 7 nm diameter nanorods with lengths 7, 30, and 60 nm. The intensity of irradiation was 0.084 mW cm^{-2}. (b) The current-voltage characteristics of 7 nm by 60 nm nanorod device exhibit rectification ratios of 10^5 in the dark and short circuit current of 0.019 mA cm^{-2} under illumination of 0.084 mW cm^{-2} at 515 nm. (c) Solar cell characteristics of 7 nm by 60 nm nanorod device illuminated with simulated AM 1.5 global light, produce a short circuit current of 5.7 mA cm^{-2}. (d) Photocurrent spectra for two devices with 60 nm long nanorods with diameters 3 and 7 nm. Reprinted with permission from Ref. [36]

yielding nanocrystals of rod like morphologies [30]. Since then numerous reports were published for synthesizing semiconducting nanocrystals of various morphologies and structure and their application in organic solar cells [31–35]. Figure 4 presents transmission electron micrographs (TEM) of representative different aspect ratio CdSe nanocrystals which have been used in organic solar cells.

It was observed that the shape directionality of these nanocrystals plays an important role in charge transport to cathode in photovoltaic devices. The use of nanorods and tetrapods of CdSe with P3HT and MEH-PPV, respectively presented power conversion efficiencies of 1.8% [35–37]. Figure 5 presents the External Quantum Efficiency (EQE) and current- voltage response of solar cells built by using different aspect ratio CdSe nanorods. We can clearly observe enhanced EQE and power conversion efficiencies with the use of high aspect ratio CdSe nanorods. The biggest problem in these devices is maintaining the solubilization of long nanorods. As the nanorods become longer, they show improved transport characteristics, but moving further towards nanowire regime it becomes increasingly difficult to solubilize them which can result in phase separation and deteriorate the device performance. Owing to the lower solubility of high aspect ratio nanorods in non polar organic solvents and a need to maintain a smooth interface, a solvent mixture of chloroform and pyridine was developed for obtaining smooth films of polymer nanocrystal composite. The weak binding Lewis base, pyridine, has a boiling point of 116 °C and acts as a ligand as well as solvent for nanocrystals while chloroform acts as a solvent for the polymer (P3HT). However, this solvent mixture needs to be optimized, as excess pyridine causes the polymer to precipitate.

Huynh et al. carried out a series of experiments and optimized conditions for smoother films of CdSe-nanorod-P3HT composites [38]. They observed that the surface roughness obtained by Atomic Force Microscope in tapping mode (AFM-TM) images relates to the phase separation. By operating AFM in tapping mode, one can identify local differences in the composition of the film by comparing the phase and the topography image. Figure 6 presents AFM-TM topography and phase image for 8 nm by 13 nm CdSe nanorod-P3HT blend films, spun from two different pyridine concentrations.

For low pyridine concentrations, the topography of these images reveals a very rough surface, while higher, i.e. ∼8 vol.% pyridine, yields smoother films. Figure 7 presents the variation of surface roughness

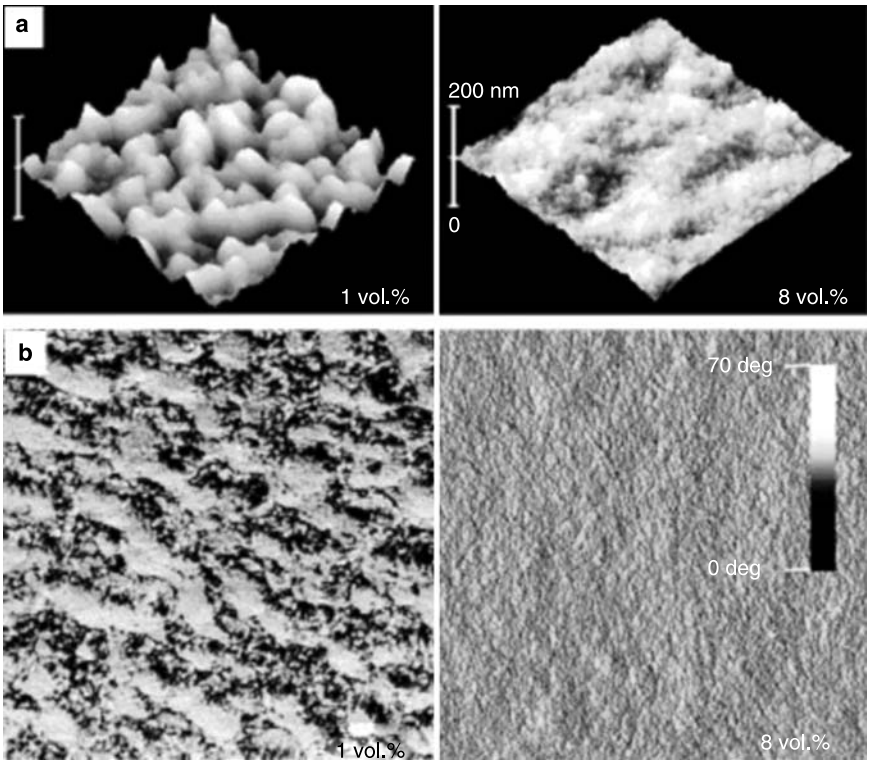

Fig. 6. AFM-TM (a) Topography and (b) phase images of films consisting of 90 wt.% 8 nm by 13 nm CdSe nanocrystals dispersed in P3HT, spin cast from 1 to 8 vol.% pyridine in chloroform. All the images are 5 μm by 5 μm. Reprinted with permission from Ref. [38]

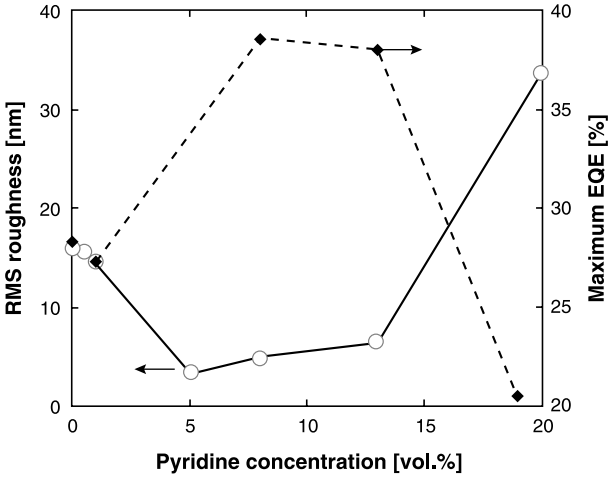

Fig. 7. Surface roughness (*open circles*) of films containing 90 wt.% of 8 nm by 13 nm CdSe nanocrystals dispersed in P3HT, spin cast from various concentrations of pyridine in chloroform. The maximum EQE (*solid diamonds*) is shown of devices made from these films. Reprinted with permission from Ref. [38]

and resulting EQE as a function of pyridine concentration used for casting composite films. We can see that the EQE initially increases with the increase of pyridine in the solvent mixture and after 15 vol.% pyridine it starts to drop down. The root-mean-square (RMS) roughness, however, shows an opposite trend with increase in pyridine concentration. The EQE, which is the percentage of electrons collected per incident photon, can be used to measure the efficiency of charge separation when the experiments are carried out under identical conditions. Separation of charges only occurs for excitons that are created within the exciton diffusion distance range of a nanocrystal-polymer interface. As better nanocrystal dispersion is achieved, single material domain sizes are smaller, and a higher EQE is achieved.

Figure 7 shows the pyridine dependence of the EQE under 0.1 mW cm^{-2} illumination for blends of 8 nm by 13 nm CdSe nanocrystals and P3HT. The maximum EQE of 35% was found to be at pyridine concentration of 8% in the solvent mixture. In comparison, the dependence of the EQE with roughness is found to show an inverse dependence: the highest EQE is reached close to lowest RMS film roughness, which corresponds to lowest phase separation, whereas for high film roughness the EQE is significantly reduced. Usually for a fixed nanocrystal concentration, the optimal solvent composition is determined by surface to volume ratio of the nanocrystal. As an example, for a device comprised of 3 nm by 100 nm CdSe nanorods, the best devices are cast from solutions containing 12 vol.% pyridine, whereas, devices with 7 and 60 nm CdSe nanorods have less surface to volume ratio and require only 4 vol.% pyridine. This is probably because more pyridine is required to maintain the surface of thinner rods covered with pyridine, as these bound pyridine molecules are in dynamic equilibrium with free pyridine in solution. Thus one needs to optimize solvent combinations for every nanocrystal system under investigation for better dispersion and efficient device performance.

In a recent report by Sun et al. power conversion of 2.1% was obtained in these nanocrystal-polymer hybrids [39]. The improved performance resulted from a vertically segregated blend configuration, similar to a bilayer configuration, where a tetrapod rich layer aligns near the top electrode (cathode) while a polymer rich layer is present at the bottom (anode). Such a configuration was achieved by spin coating the films from a solvent which evaporates slowly, allowing a vertical phase separation which thereby permits more efficient transport of charges to the electrodes, without the need of short circuit pathways responsible for lowering the open circuit voltage.

From material point of view CdTe nanocrystals present another alternative to be used in polymer nanocrystal hybrid solar cells. Most of the organic semiconductors, as well as CdSe, absorb light in the visible range, whereas as shown in Fig. 2, the sun emits radiation from 300 to 2100 nm approximately, and the desirable nanocrystal should be the one which can absorb as much as possible in the red region of the electromagnetic radiation. The bulk absorption edge of CdTe is at 820 nm, where most of the photon flux of sun's radiation is centered and it is believed that light harvesting in the vicinity of this wavelength can increase the power conversion efficiency by at least 20%, over that achieved in case of CdSe-P3HT solar cells [40]. The solar cells were built using blends of CdTe nanorods and MEH-PPV but a very low power conversion efficiency of 0.05% was achieved [41]. The reason for the low efficiency was attributed to an in efficient percolation network, agglomeration of nanoparticles, and big phase separation in composite films.

The same idea of using the maximum part of solar radiation in photocurrent generation was applied by incorporating PbS and PbSe nanocrystal in polymer matrixes [42–45]. The bulk band gap of PbS and PbSe is 0.37 and 0.26 eV respectively indicating that these

materials can cover almost up to all NIR radiation of sunlight. However, using a low band gap material in these hybrid nanostructured solar cells can have a negative impact on the power conversion efficiency because of the drop in open circuit voltage caused by the lowering of the LUMO (or band gap) of the electron acceptor moiety. In a conventional p–n junction solar cell, decreasing the energy gap below 1.0 eV reduces the open circuit voltage at a much faster rate than the increase in short circuit current due to increased absorption of light, which eventually results in a decrease in power conversion efficiency of the device [46, 47]. Thus, although the use of low band gap nanoparticles such as PbS, PbSe helps in improving the photocurrent generation up to the NIR region, it also tends to decrease the open circuit voltage. The result of which is a compromise in device performance. The experimental results suggest that the power conversion efficiencies achieved in these nanocrystal based devices were very low but the results demonstrate that near infrared radiation was successfully utilized for light harvesting experiments.

It was recently reported that colloidal PbSe and PbS quantum dots can produce up to three to seven excitons per photon, when irradiated at photon energies 4 to 7.8 times the quantum dot's band gap, indicating that these materials can be more efficient in utilization of quanta in visible radiation producing multiple excitons in addition to harvesting the IR radiation of sunlight [48–51]. The possibility to generate multiple excitons in PbS/PbSe nanocrystals indicates the possible development of an optimized and efficient photovoltaic device in the near future.

A few reports were also published for oxide based nanostructures, mainly based on ZnO [52–54] and TiO_2 [55–58] nanoparticle-polymer composites. These nanostructures possess an advantage of being cost effective as well as environmentally friendly. These ZnO nanoparticles can be synthesized using a hydrolysis and condensation approach and as such do not need any surfactant for stabilization [59]. Thereby, the film casted by spin casting the nanoparticle-polymer solution possess nanoparticles directly in contact with the polymer enhancing the charge transfer at the interface which otherwise is an important issue because of ligands in the case in CdSe and most of the other nanocrystal based devices. The solar cells based on 5 nm ZnO nanoparticles-MDMO-PPV composites at 67 wt.% of nanoparticles produced a power conversion efficiency of 1.5% under AM 1.5 conditions [53, 54]. It was observed that the loading of ZnO between 60 to 75% do not appreciably affect the power conversion efficiencies. A higher loading of nanocrystal results in higher current density, but the open circuit voltage drops out, maintaining almost same power conversion efficiency. In another report ZnO nanocrystals were blended with P3HT but a power conversion efficiency of only 0.9% was achieved at AM 1.5 conditions [52].

Another example of an oxide based semiconductor is TiO_2, which has also been explored for use in polymer based solar cells. Reports were published in which nanoporous TiO_2 was filled with conjugated polymers – a different design concept than bulk heterojunctions. Koakley et al. prepared nanostructured TiO_2 films that had a regular and open structure with pores of approximately 10 nm using structure directing diblock copolymers. The pores were then filled by first depositing film of P3HT on top of the porous TiO_2, and then heating above its melting point [55]. Solar cells based on such infiltrated TiO_2:P3HT and a 30 nm overlayer P3HT configuration yields a power conversion efficiency of 0.45% under AM 1.5 conditions [56]. In another design concept, Nelson et al. achieved penetration of conjugated copolymer into thin porous TiO_2 films by dip coating the substrate into a polymer solution. Using a cell configuration in which the mixed TiO_2-polymer layer was sandwiched between dense TiO_2 and pure polymer layers, power conversion efficiency of 0.41% was obtained [57, 58].

A bulk heterojunction solar cell was prepared by Kwong et al. for TiO_2 nanocrystals and power conversion efficiency of 0.42% was achieved [60]. However, these cells still lag behind the CdSe based cells on device performance mainly because of the poor absorption range of devices.

Because of the very good solution processability of colloidal quantum dots, recently a new configuration based on a bilayer configuration of all inorganic semiconductor nanocrystals was presented for photovoltaic cells [61]. These cells rely completely on colloidal nanocrystals, which takes care of the limitations of low mobilities, and environmental sensitivities imposed by conjugated polymers. The mechanism for photovoltaic conversion proposed was based on donor-acceptor charge transfer. In this bilayer device, the photo excitations that probe the CdTe/CdSe experience an energetic driving force for charge transfer, with holes finding lower states in the CdTe and electrons occupying lower lying CdSe states.

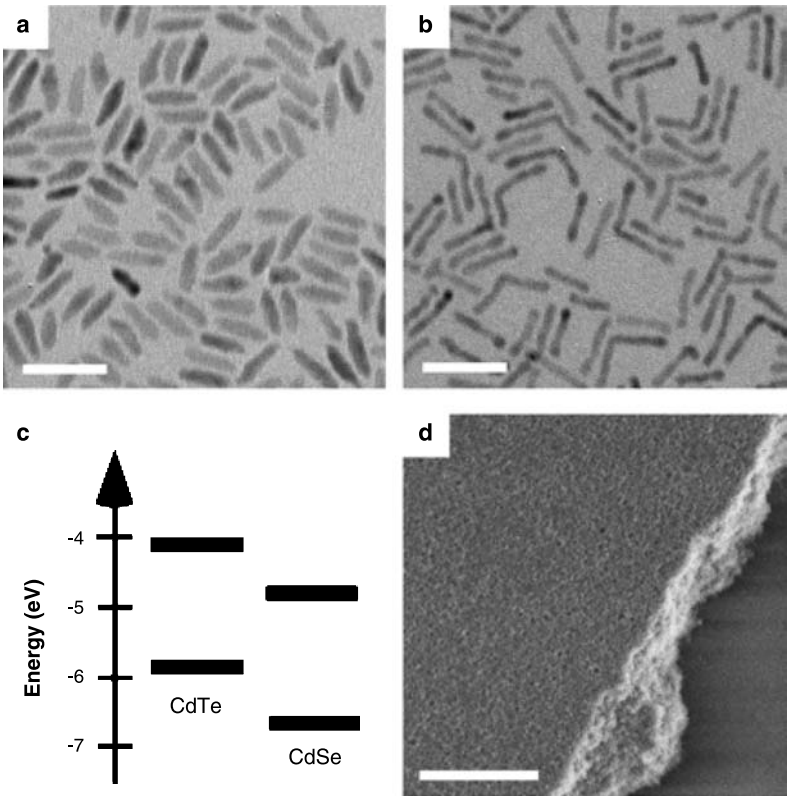

Fig. 8. Transmission electron micrographs of (a) CdSe and (b) CdTe NCs used in this investigation. Scale bar, 40 nm. (c) An energy diagram of valence and conduction band levels for CdTe and CdSe illustrates the type II charge-transfer junction formed between the two materials. Employing the effective mass approximation, bulk energy levels were modified to account for quantum confinement. Valence band edges for CdSe and CdTe rods were calculated to be −4.79 and −4.12 eV, respectively. Conduction band edges for CdSe and CdTe rods were calculated to be −6.64 and −5.85 eV, respectively. (d) A typical spin-cast film of colloidal NCs imaged by scanning electron micrography is homogeneous and defect-free; the film edge of this È100-nm film is shown for contrast with the silicon substrate. Scale bar, 1 μm. Reprinted with permission from Ref. [61]

Figure 8 presents TEM images of CdSe and CdTe nanorods used for building such a bilayer device. As shown in Fig. 8c, the energy levels of these nanorods are aligned as in type II heterojunctions, where CdSe nanorods acts as the electron acceptor while CdTe nanorods behave as the hole transporter. In such a case the carrier extraction is driven not by means of a built-in electric field from a depletion region due to substitutional dopants; rather extraction is primarily caused by directed diffusion as dictated by the type II heterojunction. These cells consist of a bilayer configuration where a layer of CdTe nanorods was first spin casted over an Indium Tin Oxide (ITO) glass coated with 2 Å alumina. The CdTe layer was then baked at high temperature to remove the surface ligands, which in this case were pyridine. After baking, another layer of CdSe nanorods was deposited. These CdSe nanorods were then baked to remove pyridine. Finally a thin Al cathode was deposited. Typical films resulting from such a casting methods are homogeneous and pinhole-free over large areas (Fig. 8d).

After photon absorption and subsequent charge transfer, the majorities of holes in CdTe readily diffuse into ITO but tend to be blocked from moving through the CdSe towards the aluminum electrode. Similarly, the majority of electrons in CdSe can only diffuse towards the Al, and not through the CdTe to ITO. The well accepted Metal-Insulator-Metal (MIM) model, in which electrodes of different workfunctions equilibrate to form a field across the dielectric active materials, likely provides an additional driving force for carrier extraction. A direct comparison of external quantum efficiencies in the CdTe only, CdSe only, and bilayer CdTe/CdSe devices showed a significant enhancement in creation and extraction of carriers due solely to the presence of a charge transfer interface within the device. As in the case of organic–inorganic hybrid solar cells, separation of electrons and holes across the interface enhances the diffusional driving force for charge extraction while reducing the possibility of exciton recombination. Devices composed of intimately mixed blends of CdSe and CdTe nanocrystals similarly exhibit enhanced quantum efficiencies over single material cells, offering further evidence that the photoaction of these devices is based on D–A junction rather than a conventional planar p–n junction.

A very fundamental distinction of this type of nanocrystal system compared to the organic solar cells is the nature of excitons. In organic solar cells it is a requirement to have a heterojunction to efficiently

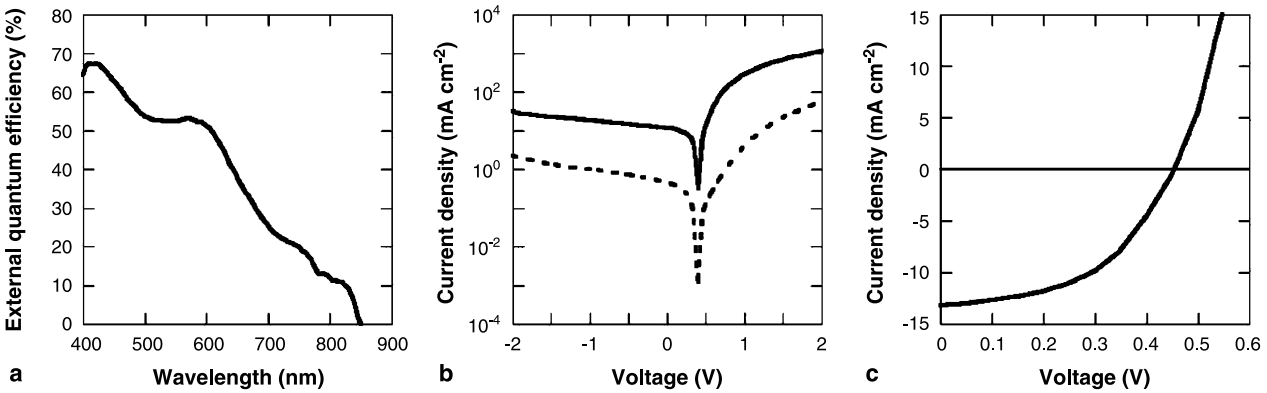

Fig. 9. (a) The normalized photoaction spectrum of a typical bilayer device after sintering reveals the broadened spectral response and enhanced quantum efficiency that result from sintering. (b) I–V characteristics of a typical bilayer device before sintering (*dotted*) and after sintering (solid), measured at simulated one-sun AM1.5G illumination. The sintered cell shows over an order of magnitude enhancement in photocurrent whereas the open-circuit voltage remains virtually unchanged. (c) The use of a Ca 20-nm/Al 80-nm top contact allows for fabrication of devices with AM1.5G power conversion efficiencies as high as 2.9%. Reprinted with permission from Ref. [61]

produce free charges from excitons but this is not the case with all nanocrystal based solar cells. Rod shaped nanocrystals with a very high aspect ratio are thought to display very weak or almost no confinement along the length of the rod [62]. Excitons can thus dissociate over this dimension, creating free carriers throughout the nanocrystal film. Thus these types of cells provide ways to counter the exciton recombination losses of typical bulk heterojunction organic solar cells.

However, with the electron and hole freely occupying the donor and acceptor materials, these carriers are more susceptible to recombination in the NC system. This recombination is facilitated by the presence of surface states on the NCs, which act as traps to carriers as they move through the film. Surface trap states can be minimized in a densely packed array of NCs, and concurrently improve carrier transport in the device, by annealing and sintering the films. Exposing the nanocrystal bilayer to a $CdCl_2$ solution and subsequent sintering at 400 °C led to an improvement of photovoltaic performance by two orders of magnitude. The photoresponse of sintered CdSe/CdTe bilayer cells indicates the drastic rise in conductivity of the active layers. External quantum efficiency up to 70% was achieved with this methodology, as displayed in Fig. 9a. By varying simple system parameters such as using Ca top capped with Al as cathode, a power conversion efficiency of up to 2.9% could be achieved in this configuration (Fig. 9b and c) under AM 1.5 solar irradiation. These solar cells have the biggest advantage of their environmental or photostability compared to usual organic solar cells. In fact, aging improved the performance of the solar cell rather than deteriorated

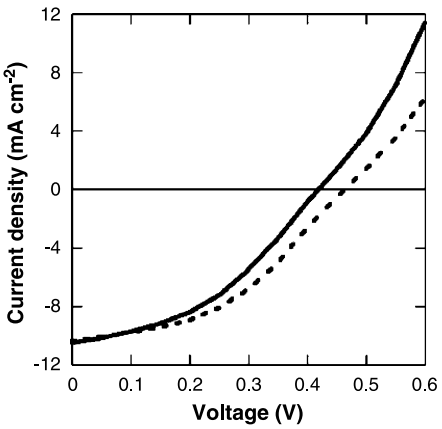

Fig. 10. I–V behavior at simulated one-sun AM1.5G illumination for a typical sintered bilayer device upon first exposure to air (*solid*) and after 13,000 h of exposure to ambient atmosphere and light at open circuit. Idle exposure to air and ambient light results in minimal degradation of photocurrent and ultimately affords a 13.6% improvement in overall power conversion efficiency. Reprinted with permission from Ref. [61]

their performance. The stability and effect of air exposure on power conversion efficiency of sintered solar cells is presented in Fig. 10, where we can clearly observe improvement in open circuit voltage as the exposure time to air is increased. These cells thereby present a new class of nanocrystal based cells which provide higher power conversion efficiency than conventional nanoparticle-polymer hybrid solar cells and are environmentally stable.

Conclusions

We presented a review of the state of art in colloidal nanocrystal based polymeric solar cells. We ob-

served that the performance of such organic solar cells is determined by an interplay between roughness/morphology of the interface between two components, morphology of nanocrystals, as well as the chemical type of nanocrystals. In addition to the fundamental question of the device absorption range, the design concept of these solar cells was also found to be important. To further improve the performance of these hybrid solar cells one needs to optimize the above mentioned parameters. Optimum performance of these cells needs high quality of nanocrystals with good material properties. A few reports were published recently for hybrid nanocrystals which show compositionally tunable properties [63–65], these materials could also be explored for future photovoltaic devices.

Acknowledgement. The Natural Sciences and Engineering Research Council of Canada is thanked for financial support.

References

1. Green M A, Emery K, King D L, Igari S, Warta W (2001) Solar cell efficiency tables. Prog Photovoltaics 9: 287
2. Scholes G D, Rumbles G (2006) Excitons in nanoscale systems. Nature Mater 5: 683
3. Choong V, Park Y, Gao Y, Mehrmeister T, Muellen K, Hseih B R, Tang C W (1996) Dramatic photoluminescence quenching of phenylene vinylene oligomer thin films upon submonolayer Ca deposition. Appl Phys Lett 69: 1492
4. Halls J J M, Pichler K, Friend R H, Moratti S C, Holmes A B (1996) Exciton diffusion and dissociation in poly (p-phenylenevinylene)/C_{60} heterojunction photovoltaic cell. Appl Phys Lett 68: 3120
5. Grozema F C, Siebbeles L D A, Gelinck G H, Warman J M (2005) The optoelectronic properties of isolated phenylenevinylene molecular wires. Top Curr Chem 257: 135
6. Halls J J M, Friend R H (1996) The photovoltaic effect in a poly(p-phenylenevinylene)/perylene heterojunction. Synth Met 85: 1307
7. Bozano L, Carter S A, Scott J C, Malliaras G G, Brock P J (1999) Temperature- and field-dependent electron and hole mobilities in polymer light-emitting diodes. Appl Phys Lett 74: 1132
8. Rispens T M, Meetsma A, Rittberger R, Brabec C J, Sariciftci N S, Hummelen J C (2003) Influence of the solvent on the crystal structure of PCBM and the efficiency of MDMO-PPV:PCBM 'plastic' solar cells. Chem Commun 17: 2116
9. Brabec C J, Nann T, Shaheen S E (2004) Nanostructured p–n junctions for printable photovoltaics. MRS Bulletin 29: 43
10. Jannsen R A J, Christians M P T, Hare C, Martin N, Sariciftci N S, Heeger A J, Wudl W (1995) Photoinduced electron transfer reactions in mixed films of π-conjugated polymers and a homologus series of tetracyano-p-quinodimethane derivatives. J Chem Phys 103: 8840
11. Kittel C (1996) Introduction to solid state physics, 6th end. John Wiley and Sons Inc., New York
12. Yu P, Cardona M (1996) Fundamentals of semiconductors. Springer, Berlin
13. Bredas J L, Cornil J, Heeger A J (1996) The exciton binding energy in luminescent conjugated polymers. Adv Mater 8: 447
14. Bjorklund T J, Lim S H, Bardeen C J (2001) Use of picosecond fluorescence dynamics as an indicator of exciton motion in conjugated polymers: dependence of chemical structure and temperature. J Phys Chem B 105: 11970
15. Friend R H, Denton R J, Halls J J M, Harrison N T, Holmes A B, Kohler A, Lux A, Moratti S C, Pichler K, Tessler N, Towns K, Wittman H F (1997) Electronic excitations in luminescent conjugated polymers. Solid State Commun 102: 249
16. Conwell E M (1996) Definition of exciton binding energy for conducting polymers. Synth Met 83: 101
17. Bassler H, Brandl V, Deussen M, Gobel E O, Kersting R, Kurz H, Lemmer U, Mahrt R F, Ochsej A (1995) Excitation dynamics in conjugated polymers. Pure Appl Chem 67: 377
18. Sariciftci N S, Heeger A J (1994) Reversible metastable, ultra fast photo induced electron transfer from semi conducting polymers to buckminsterfullerene and in the corresponding donor/acceptor hetero junctions. Int J Mod Phys B 8: 237
19. Halls J M, Cornil J, Dosantos D A, Silbey R, Hwang D H, Holmes A B, Bredas J L, Friend R H (1999) Charge- and energy-transfer processes at polymer/polymer interfaces: a joint experimental and theoretical study. Phys Rev B 60: 5721
20. Lee K H, Janssen R A J, Sariciftci N S, Heeger A J (1994) Direct evidence of photo induced electron transfer in conducting polymer-C_{60} composites by infrared photo excitation spectroscopy. Phys Rev B 49: 5781
21. Ginger D S, Greenham N S (1999) Photo induced electron transfer from conjugated polymers to CdSe nano crystals. Phys Rev B 49: 10622
22. Soos Z G, Hennessy M H, Wen G (1998) Frenkel and charge transfer states of conjugated polymers and molecules. Chem Phys 227: 19
23. Kohler A, doSantos D A, Belijonne D, Shuai Z, Bredas J L, Holmes A B, Kraus A, Mullen K, Friend R H (1998) Charge separation in localized and delocalized electronic states in polymeric semiconductors. Nature 392: 903
24. Rodriguez Monge L (1998) Charge separation in organic semiconductor composites. 2. Study of the ground state and low lying excited states involved. J Phys Chem B 102: 4466
25. Ginger D S, Greenham N C (1999) Charge separation in conjugated-polymer/nanocrystal blends. Synth Met 101: 425
26. Leatherdale C, Kagan C R, Morgan N Y, Empedocles S A, Kastner M A, Bawendi M G (2000) Photoconductivity in CdSe quantum dot solids. Phys Rev B 62: 2669
27. Bozano L, Carter S A, Scott J C, Malliaras G G, Brock P J (1999) Temperature- and field- dependent electron and hole mobilities in polymer light emitting diodes. Appl Phys Lett 74: 1132
28. In ASTM standard table for reference solar spectral irradiances G 179-03, www.astm.org, 2003
29. Greenham N C, Peng X, Alivisatos A P (1996) Charge separation and transport in conjugated-polymer/semiconductor-nanocrystal composites studeied by photoluminescence quenching and photoconductivity. Phys Rev B 54: 17628
30. Peng X, Manna L, Yang W, Wickham J, Scher E, Kadavanich A, Alivisatos A P (2000) Shape control of CdSe nanocrystals. Nature 404: 59–61
31. Peng Z A, Peng X (2001) Mechanisms of shape evolution of CdSe nanocrystals. J Am Chem Soc 123: 1389
32. Manna L, Scher E, Alivisatos A P (2000) Synthesis and soluble processable rod-, arrow-, teardrop-, and tetrapod-shaped CdSe nanocrystals. J Am Chem Soc 122: 12700
33. Kumar S, Ade M, Nann T (2005) Synthesis and structural metastability of CdTe nanowires. Chem Eur J 11: 2220

34. Kumar S, Nann T (2003) Hexagonal CdTe nanoparticles of various morphologies. Chem Commun 19: 2478
35. Sun B, Marx E, Greenham N C (2003) Photovoltaic devices using blends of CdSe nanoparticles and conjugated polymers. Nano Lett 3: 961
36. Huynh W U, Dittmer J J, Alivisatos A P (2002) Hybrid nanorod-polymer solar cells. Science 295: 2425
37. Liu J, Tanaka T, Sivula K, Alivisatos A P, Frechet J M (2004) Employing end-functional polythiophene to control the morphology of nanocrystal-polymer composites in hybrid solar cells. J Am Chem Soc 126: 6550
38. Huynh W U, Dittmer J J, Libby W C, Whitting G L, Alivisatos A P (2003) Controlling the morphology of nanocrystal-polymer composites for solar cells. Adv Funct Mater 13: 73
39. Sun B, Snaith H J, Dhoot A S, Westenhoff S, Greenham N C (2005) Vertically segregated hybrid blends for photovoltaic devices with improved efficiency. J. Appl. Phys 97: 014914-1
40. Huynh W U (2003) PhD Thesis, University of California
41. Kumar S, Nann T (2004) First solar cells based on CdTe nanoparticle/MEH-PPV composites. J Mater Res 19: 1990
42. Guenes S, Fritz K P, Neuberger H, Sariciftci N S, Kumar S, Scholes G D (2006) Hybrid solar cells using PbS nanoparticles. Solar Energy Mat Solar Cells (in press)
43. McDonald S, Konstantatos G, Zhang S, Cyr P W, Klem E J D, Levina L, Sargent E H (2005) Solution processed PbS quantum dot infrared detectors and photovoltaics. Nature Mat 4: 138
44. Qi D, Fischbein M, Drndic M, Selmic S (2005) Efficient polymer-nanocrystal quantum dot photodetectors. Appl Phys Lett 86: 093103
45. Chaudhari K R, Sahoo Y, Ohulchansky T Y, Prasad P N (2005) Efficient photoconductive devices at infrared wavelengths using quantum dot-polymer nanocomposites. Appl Phys Lett 87: 073110
46. Shockley W, Queisser H J (1961) Detailed balance limit of efficiency of p–n junction solar cells. J Appl Phys 32: 510
47. Prince M B (1955) Silicon solar energy converters. J Appl Phys 26: 534
48. Schaller R D, Sykora M, Pietryga J M, Klimov V I (2006) Seven excitons at the cost of one: redefining the limits for conversion efficiency of photons into charge carriers. Nano Lett 6: 424
49. Schaller R D, Agranovich V M, Klimov V I (2005) High efficiency carrier multiplication through direct photogeneration of multi excitons via virtual single exciton states. Nature Phys 1: 189
50. Ellinson R, Beard M, Johnson J, Yu P, Micic O, Nozik A, Shabaev A, Efros A (2005) Highly efficient multiple exciton generation in colloidal PbSe and PbS quantum dots. Nano Lett 5: 865
51. Schaller R D, Klimov V I (2004) High efficiency carrier multiplication in PbSe nanocrystals: Implications for solar energy conversion. Phys Rev Lett 92: 186601
52. Beek W J E, Wienk M M, Janssen R A J (2006) Hybrid solar cells from regioregular polythiophene and ZnO nanoparticles. Adv Func Mater 16: 1112
53. Beek W J E, Wienk M M, Janssen R A J (2004) Efficient solar cells from zinc oxide nanoparticles and a conjugated polymer. Adv Mater 16: 1009
54. Beek W J E, Wienk M M, Janssen R A J (2005) Hybrid polymer solar cells based on zinc oxide. J Mater Chem 15: 2985
55. Koakley K, Liu Y, McGehee M D, Frindell K L, Stucky G D (2003) Infiltrating semiconducting polymers into self assembled mesoporous titania films for photovoltaic applications. Adv Func Mater 13: 301
56. Koakley K, McGehee M D (2003) Photovoltaic cells made from conjugated polymers infiltrated into mesoporous titania. Appl Phys Lett 83: 3380
57. Ravirajan P, Haque S A, Durrant J R, Poplavskyy D, Bradley D D C, Nelson J (2004) Hybrid nanocrystalline TiO_2 solar cells with a fluorine-thiophene copolymer as a sensitizer and hole conductor. J Appl Phys 95: 1473
58. Ravirajan P, Haque S A, Durrant J R, Bradley D D C, Nelson J (2005) The effect of polymer optoelectronic properties on the performance of multilayer hybrid polymer/TiO_2 solar cells. Adv Func Mater 15: 609
59. Pacholski C, Kornowski A, Weller H (2002) Self assembly of ZnO: from nanodots to nanorods. Angew Chem Int Ed 41: 1188
60. Kwong C Y, Djurisic A B, Chui P C, Cheng K W, Chan W K (2004) Influence of solvent on film morphology and device performance of poly(3-hexylthiophene): TiO_2 nanocomposite solar cells. Chem Phys Lett 384: 372
61. Gur I, Fromer N A, Geier M A, Alivisatos A P (2005) Air-stable all-inorganic nanocrystal solar cells processed from solution. Science 310: 462
62. Li L S, Hu J T, Yang W D, Alivisatos A P (2001) Band gap variation of size- and shape-controlled colloidal CdSe quantum rods. Nano Lett 1: 349
63. Milliron D J, Hughes S M, Cui Y, Manna L, Li J, Wang L-W, Alivisatos A P (2004) Colloidal nanocrystal heterostructures with linear and branched morphology. Nature 430: 190
64. Kudera S, Carbone L, Casula M F, Cingolani R, Falqui A, Snoeck E, Parak W J, Manna L (2005) Selective growth of PbSe on one or both tips pf colloidal semiconductor nanorods. Nano Lett 5: 445
65. Cozolli P D, Pellegrino T, Manna L (2006) Synthesis, properties and perspectives of hybrid nanocrystal structures. Chem Soc Rev 35: 1195